Supplemental Table 1. Listing of Mice Used in this Analysis

SHORT-TERM IMMUNIZATION PROTOCOL

	CEP / MSA	CFA	Naïve	MSA	Rag- / - / CEP	Rag- / - / naïve
Mice immunized	64	15	N/A (15)	18	5	N/A (6)
Mice harvested	62	14	15	18	5	6
Eye (OS) fixed in Glut/Form	62	14	15	18	5	6
Eye (OD) frozen in OCT	62	14	15	18	5	6
Kidney (OCT)	15		5	5		
Kidney (paraformaldehyde)	28	10	5	18		
Brain (OCT)	15		5	5		
Spleen / lymph nodes	10	5	5	5	5	5
Analysis of tissue:						
ELISA - Antibody titer	62	14	15	18	3	6
ELISPOT	5		5	5	5	5
Histopathology (eye-OS)	62	14	15	18	5	5
Histopathology (kidney)	5	3	3	5		
Measurement of basal laminar deposits	5	5	5	5	4	4
C3d Immunohistochemistry (eye-OD)	5	5	5	5	3	3

LONG-TERM IMMUNICATION PROTOCOL

Mice immunized	20	8	N/A (6)	6	5	N/A (5)
Mice harvested	20	8	6	6	5	5
Eye (OS) fixed in Glut/Form	20	8	6	6	5	5
Eye (OD) frozen in OCT	20	8	6	6	5	5
Kidney (OCT)	5		3	5		
Brain (OCT)	5		3	5		
Spleen / lymph nodes	10		5	5	5	5
Analysis of tissue:						
ELISA - Antibody titer	20	8	6	6	5	5
ELISPOT	5		5	5	5	5
Histopathology	20	8	6	6	5	5
Measurement of basal laminar deposits	8	3	3	3	3	3
C3d Immunohistochemistry	3	3	3	3		

Supplemental Table 1. Listing of mice used in this analysis. Mice included here are of the C57BL/6 strain. An additional 85 BALB/C mice were also immunized but their responses to CEP-MSA were not as robust as in the C57BL/6 mice and are not included here.

Supplemental Fig. 1

Histology of the Naïve Mouse RPE

Title: Oxidative damage induced inflammation initiates age-related macular degeneration

Authors: JG Hollyfield, VL Bonilha, ME Rayborn, X Yang, KG Shadrach, L Lu, RL Ufret, RG Salomon and VL Perez

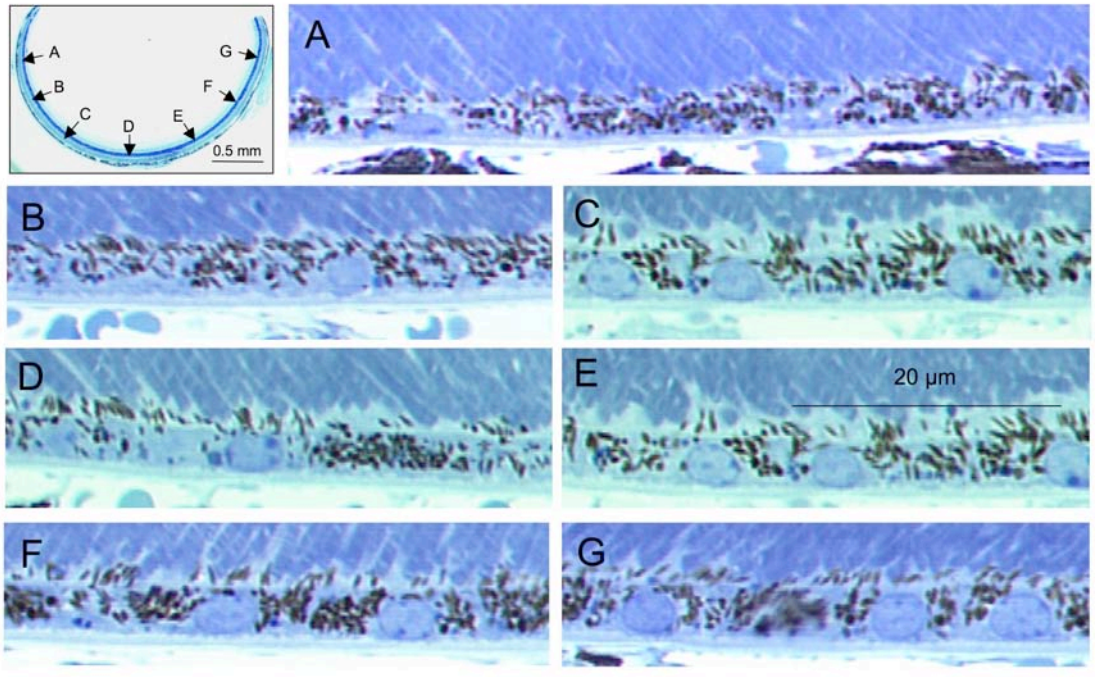

Supplemental Fig. 1. Section through the fundus of the eye of a 6 month old naïve mouse used to define the normal RPE histology. The low magnification image in the upper left shows the entire eye from superior (right) to inferior (left) margin. The letters from A to G above arrows in this low magnification image indicate the location where the higher magnification images labeled (A-G) were taken. The tips of the photoreceptor outer segments are located along the top of each image. The RPE, containing dark melanin granules, is intact with no suggestion of any pathological changes. Compare this RPE with the changes present in Supplemental Figs. 2-4. Enlargments (A-G) photographed and presented at identical magnifications. Magnification scale is in (E).

Supplemental Fig. 2

Histology of a CEP-MSA Immunized Mouse with Minor RPE Pathology

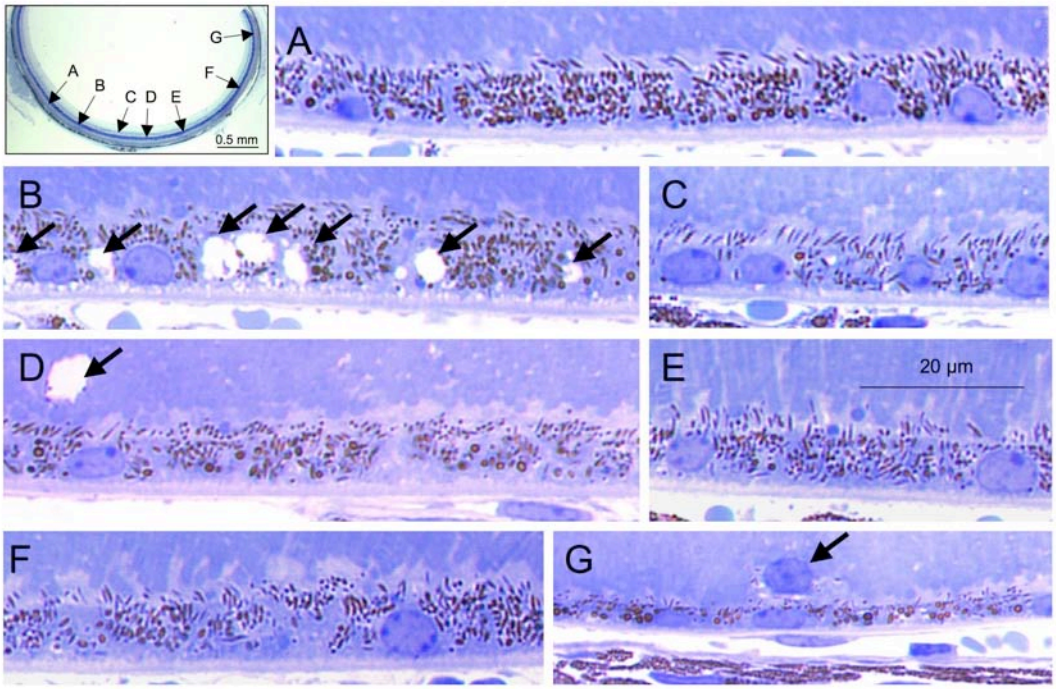

Supplemental Fig. 2. Section from the eye of an MSA-CEP immunized mouse from the short-term recovery protocol with changes in the outer retina defined as "minor" RPE pathology. The low magnification image in the upper left shows the complete section along the midline of the eye from superior (right) to inferior (left) margin. The letters from A to G above arrows in this low magnification image in the upper left indicate the location of the higher magnification images labeled (A) through (G). In the enlargements, the tips of the photoreceptor outer segments are located along the top of each image. Pathology is present in locations (B), (D) and (G) in the low magnification image at upper left. These included vesiculation of RPE cells (B, at arrows), a large lesion in the IPM (D, at arrow), and an invading cell containing melanin in the IPM (G, at arrow). The RPE in (A), (C), (E) and (F) appears normal. Compare with RPE in Supplemental Figures 2, 3 and 4.

Supplemental Fig. 3

Histology of a CEP-MSA Immunized Mouse with Moderate RPE Pathology

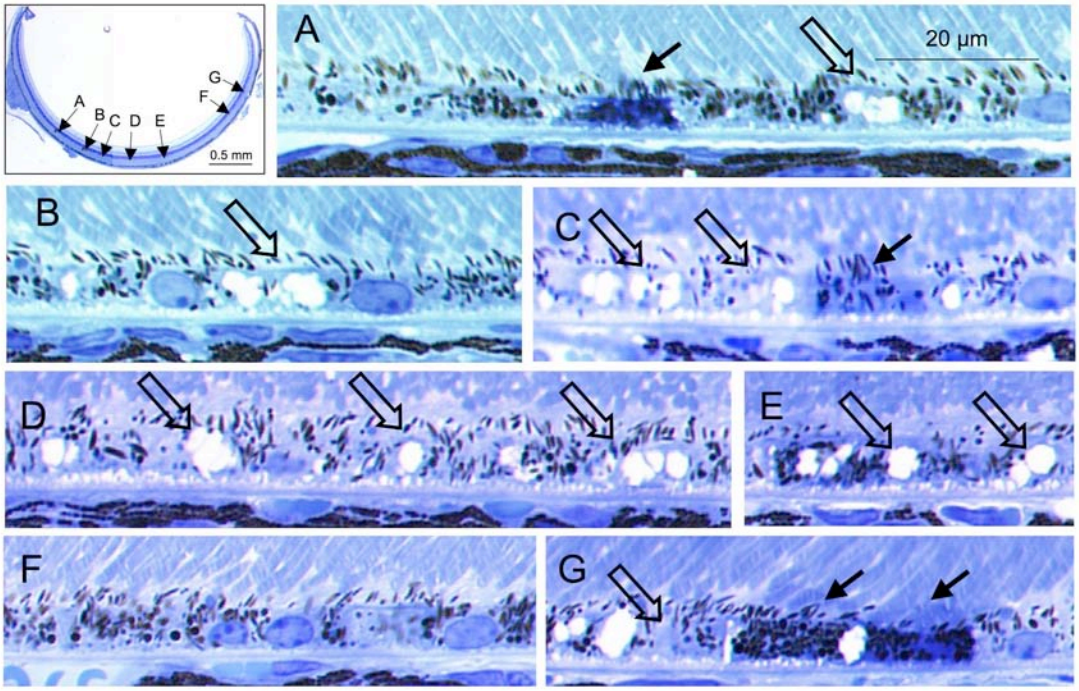

Supplemental Fig. 3. Section through the fundus of the eye of a CEP-MSA immunized mouse from the short-term recovery protocol with changes in the outer retina defined as "moderate" RPE pathology. The low magnification image in the upper left shows the complete section along the midline of the eye from superior (right) to inferior (left) margin. The letters A to G above arrows in this low magnification image indicate the location of the higher magnification fields labeled (A-G). The tips of the photoreceptor outer segments are located along the top of each enlargment image. Pathological changes in the RPE are present in each enlargement images presented except for (F), where the RPE appears normal. These changes include pyknotic RPE cells, (the intense staining cells in (A), (C) and (G), indicated by solid arrows). Vesiculation of RPE cells is evident in (A), in (B), (C), (D), (E) and (G) open arrows. Areas not photographed at higher magnification contained normal RPE similar to that shown in (F). Enlargments (A-G) photographed and presented at identical magnifications. Magnification bar is presented in (A).

Supplemental Fig. 4

Histology of a CEP-MSA Immunized Mouse with Severe RPE Pathology

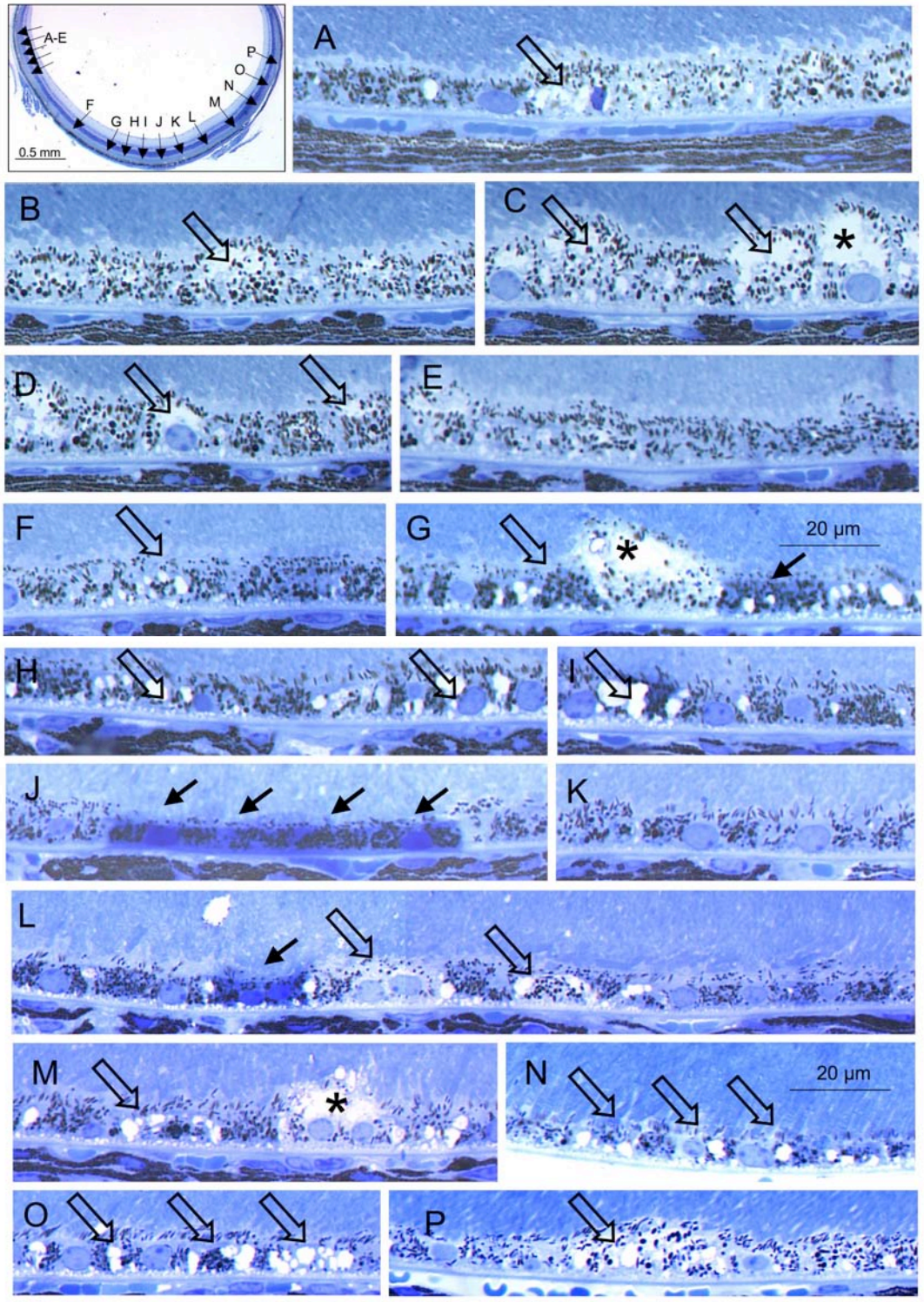

Supplemental Fig. 4. Section from the eye of a CEP-MSA immunized mouse from the short-term recovery protocol with changes in the outer retina that were defined as "severe" RPE pathology. The 17 arrows labeled A–P in the low magnification image in the upper left indicate areas of pathology photographed and presented in the enlargement images with corresponding letters. Pathology evident include RPE vesiculation [(A-I), (L-P) open arrows], RPE lysis [(C), (G) and (M) asterisks (*)], and RPE pyknosis [(J), and (L) solid arrows]. A short length of RPE between (E) and (F) shows normal morphology. Enlargments (A-P) were photographed and presented at identical magnifications. Magnification scale is presented in (G) and (N).

Supplemental Fig. 5

Fundus Photographs from Naïve and CEP-MSA Immunized Mice

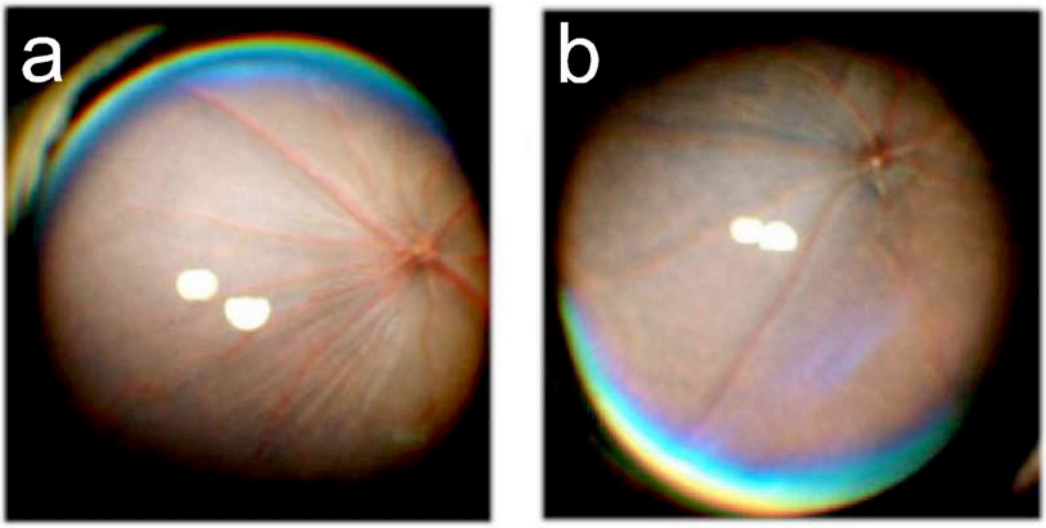

Supplemental Fig. 5. Photographs of the fundus from the right eye of two 9 month old C57BL/6 mice. (a) is from a naïve mouse and (b) is from a mouse immunized with CEP-MSA seven months earlier. Note the mottled background throughout the fundus in (b) that is absent in (a). These pigmentary changes may be caused by basal laminar deposits below the RPE shown in **Fig. 4** and also in **Supplemental Fig. 6.**

Supplemental Fig. 6

Histology of a CEP-MSA Immunized Mouse from Long-term Recovery Protocol Showing the Extent of Basal Laminar Deposits

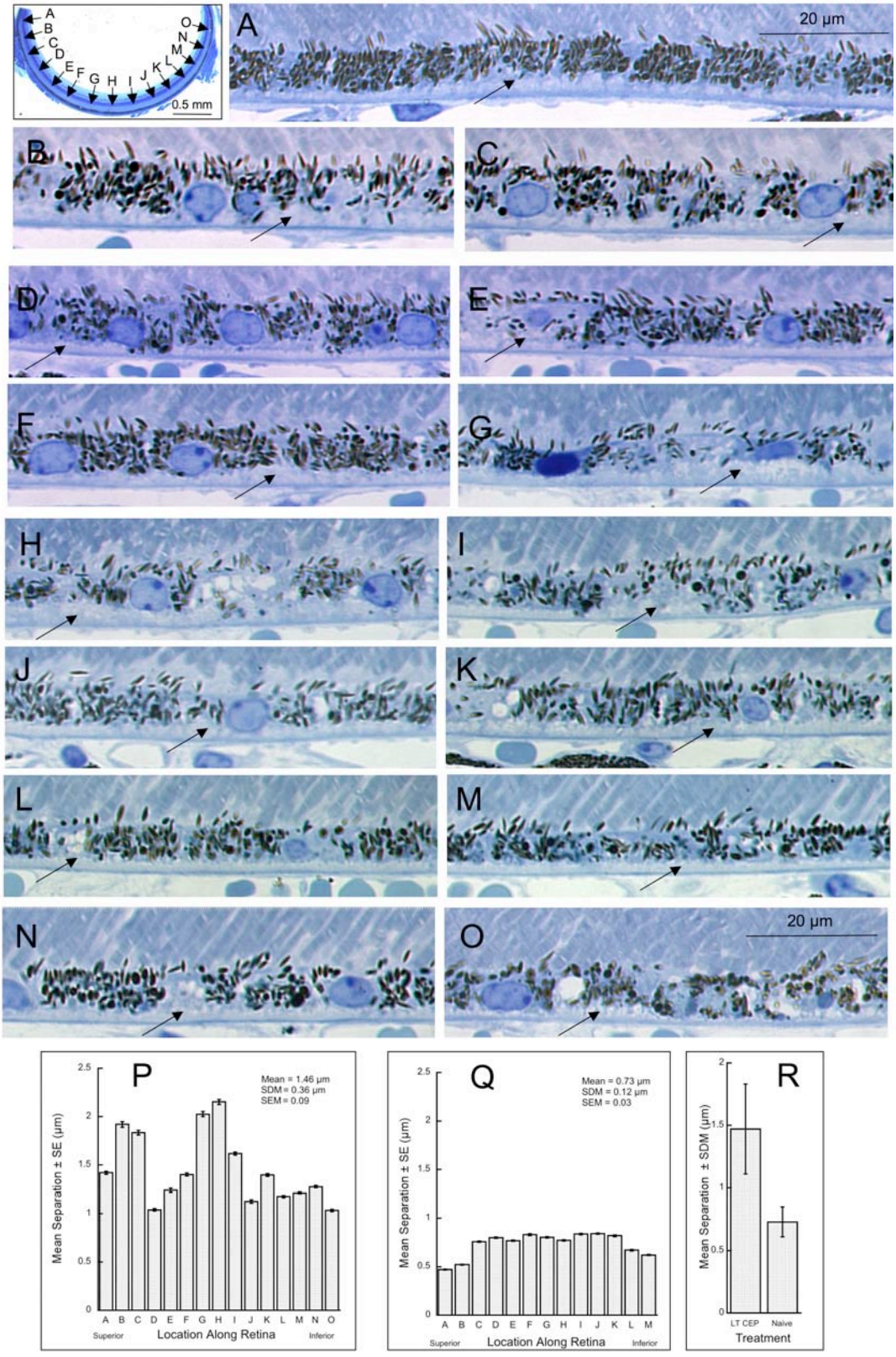

Supplemental Fig. 6. Section from the eye of a CEP-MSA immunized mouse from the long-term recovery protocol illustrating extent and intraocular variability of basal laminar deposits presented in **Fig. 4**. In the low magnification image in the upper left, arrows labeled from (A) through (O) are located at 400 μm intervals from the superior (left) to inferior (right) margin. In the higher magnification images presented, in each of these positions (A through O, respectively) small arrows indicate the location of the basal laminar deposits that are present throughout the expanse of the sub-RPE compartment with variable thickness. For example compare the thickness of the sub-RPE compartment at the arrow in (D) with the thickness at the arrow in (G). We measured the separation distance between Bruch's membrane across this debris zone to the edge of the RPE cytoplasm containing melanin at each pixel location across the full image (an expanse of 130 μm). A mean value was established for each image and graphic representation of these data are presented in (P). Note that the separation distance shows two fold variation between minimum at position (O) and maximum at position (H). The variation in the displacement measurements below the RPE in this example from a long-term CEP-immunized mouse is compared to the data from identical measurements of the sub-RPE compartment in the eye of a naïve mouse recovered at an identical age. These histograms are presented in (Q). (Photos measured from the naïve mouse eye are not shown.) Notice that the displacement values are lower at superior (location A and B) and inferior (location M and L) margin but are similar in deeper locations. Each mean separation in the normal mouse histogram presented in (Q) is substantially lower than the displacement mean at any location in the histogram presented in (P). The mean displacement values for the entire data set from these tissues are compared in (R).

Supplemental Fig. 7

Comparison of CEP-MSA and CEP-BSA as Coating Antigens for ELISA Assays

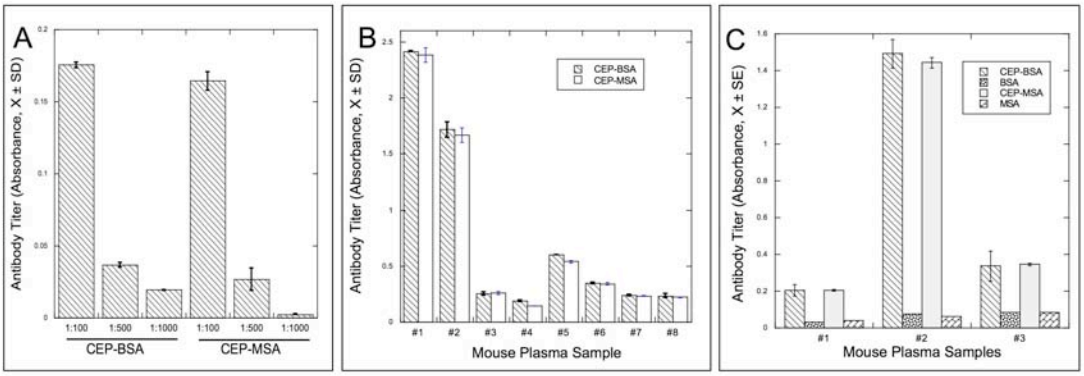

Supplemental Fig. 7. Preliminary studies were conducted to establish the efficiency of CEP-BSA versus CEP-MSA as coating antigen used in ELISA assays of CEP-antibody levels in mouse plasma immunized with CEP-MSA. In (A) serial dilutions of mouse plasma were used in ELISA wells coated with either CEP-BSA or CEP-MSA. At the higher dilutions (1:100), the absorbance values are similar between each coating agents, but at lower dilutions (1:1000) the CEP-BSA shows higher absorbance values. In (B) CEP-antibody titers in plasma samples from eight mice immunized with CEP-MSA at 1:100 dilution levels were directly evaluated with ELISA using CEP-BSA and CEP-MSA as coating antigen. While major differences are evident between the individual samples, the absorbance values between the paired comparisons of each plasma sample are virtually identical. In (C) comparisons are made with plasma from CEP-MSA immunized mice to address the issue of an immune response to the protein (MSA) versus the CEP-adduct (CEP-MSA). Note that only minor background levels of absorbance were obtained when either MSA or BSA were used as the coating agent. These minor absorbance levels (< 0.1) represent background. These comparisons strongly indicated that the immune response in mice immunized with CEP-MSA is directed toward the CEP-adduct and not to the MSA carrier protein.